



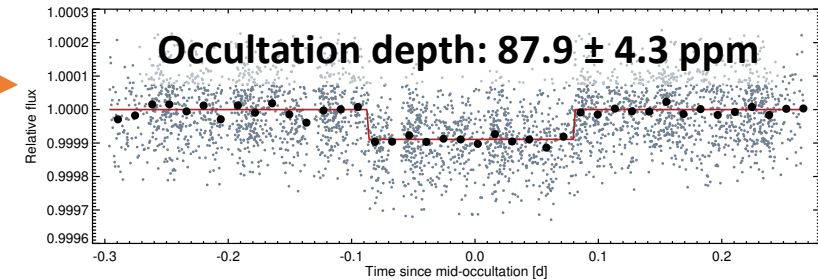
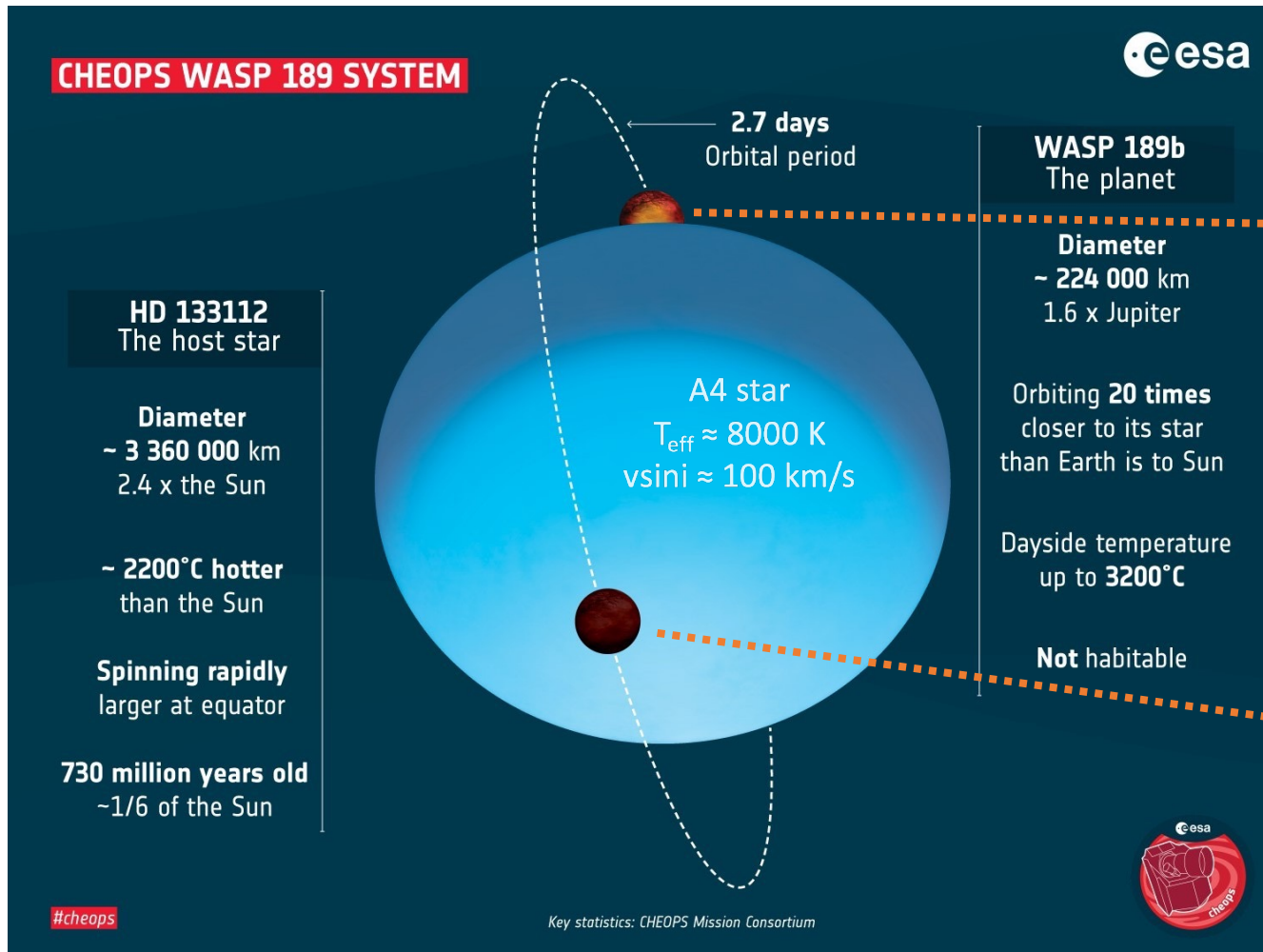
# The atmosphere and architecture of WASP-189 b probed by its **CHEOPS** phase curve

Adrien Deline (*University of Geneva*)

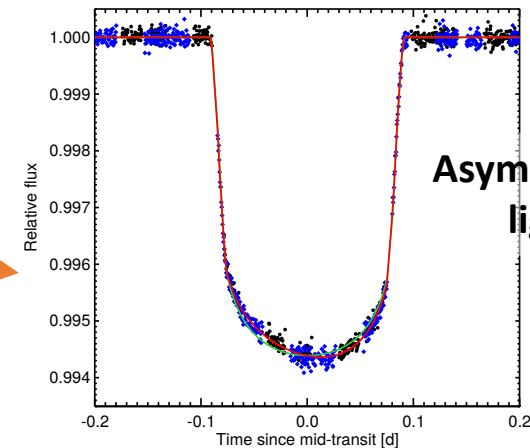
M. J. Hooton, M. Lendl, B. Morris, S. Salmon, G. Olofsson, C. Broeg, D. Ehrenreich, M. Beck, A. Brandeker, S. Hoyer, S. Sulis, V. Van Grootel, V. Bourrier, O. Demangeon, B.-O. Demory, K. Heng, H. Parviainen, L. M. Serrano, V. Singh, A. Bonfanti, L. Fossati, D. Kitzmann, S. G. Sousa, T. G. Wilson and the CHEOPS consortium

# WASP-189 planetary system

Discovery paper: Anderson et al. (2018)  
CHEOPS observations: Lendl et al. (2020)



Lendl et al. (2020)



Lendl et al. (2020)

# Gravity-darkened stellar photosphere

- Rapid rotation leads to non-negligible centrifugal force near the equator

- Effective surface gravity is affected:

$$\vec{g}_{\text{eff}}(\vartheta) = -\frac{GM_{\star}}{r_{\vartheta}^2} \vec{u}_r + \left(\frac{2\pi}{P_{\star}}\right)^2 R_{\star} \sin(\vartheta) \vec{u}_{\star}$$

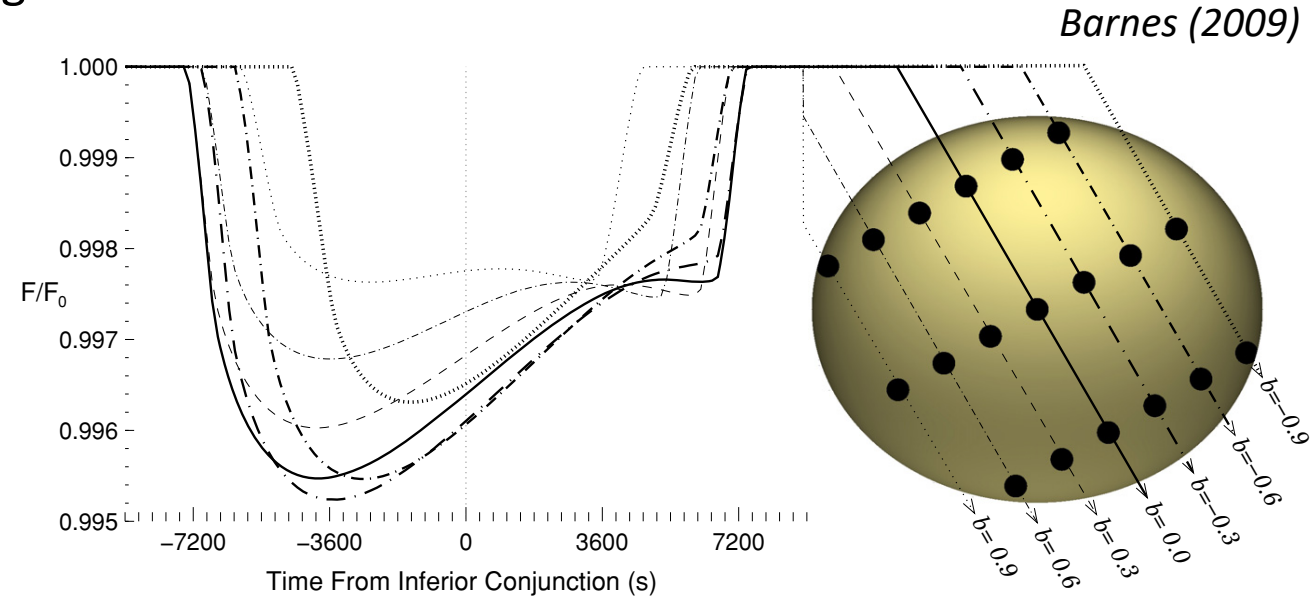
- Effect on local temperature (e.g. Maeder 2009):

$$T(\vartheta) = T_{\text{pole}} \left( \frac{g_{\text{eff}}(\vartheta)}{g_{\text{eff,pole}}} \right)^{\beta}$$

- Local brightness changes from stellar poles to equator → gravity darkening

- Asymmetric transit light curve

→ access to star-planet relative orientation:  $\Psi_p = \arccos[\cos(i_p) \cos(i_{\star}) + \cos(\lambda_p) \sin(i_p) \sin(i_{\star})]$



## The atmosphere and architecture of WASP-189 b probed by its CHEOPS phase curve

A. Deline<sup>1,\*</sup>, M. J. Hooton<sup>2</sup>, M. Lendl<sup>1</sup>, B. Morris<sup>3</sup>, S. Salmon<sup>1</sup>, G. Olofsson<sup>4</sup>, C. Broeg<sup>2,3</sup>, D. Ehrenreich<sup>1</sup>, M. Beck<sup>1</sup>, A. Brandeker<sup>4</sup>, S. Hoyer<sup>5</sup>, S. Sulis<sup>5</sup>, V. Van Grootel<sup>6</sup>, V. Bourrier<sup>1</sup>, O. Demangeon<sup>7,8</sup>, B.-O. Demory<sup>3</sup>, K. Heng<sup>3,9,10</sup>, H. Parviainen<sup>11,12</sup>, L. M. Serrano<sup>13</sup>, V. Singh<sup>14</sup>, A. Bonfanti<sup>15</sup>, L. Fossati<sup>15</sup>, D. Kitzmann<sup>3</sup>, S. G. Sousa<sup>7</sup>, T. G. Wilson<sup>16</sup>, Y. Alibert<sup>2</sup>, R. Alonso<sup>11,12</sup>, G. Anglada<sup>17</sup>, T. Bárczy<sup>18</sup>, D. Barrado Navascues<sup>19</sup>, S. C. C. Barros<sup>7,8</sup>, W. Baumjohann<sup>15</sup>, T. Beck<sup>2</sup>, A. Bekkelien<sup>1</sup>, W. Benz<sup>2,3</sup>, N. Billot<sup>1</sup>, X. Bonfils<sup>20</sup>, J. Cabrera<sup>21</sup>, S. Charnoz<sup>22</sup>, A. Collier Cameron<sup>16</sup>, C. Corral van Damme<sup>23</sup>, Sz. Csizmadia<sup>21</sup>, M. B. Davies<sup>24</sup>, M. Deleuil<sup>5</sup>, L. Delrez<sup>25,6</sup>, T. de Roche<sup>2</sup>, A. Erikson<sup>21</sup>, A. Fortier<sup>2,3</sup>, M. Fridlund<sup>26,27</sup>, D. Futyan<sup>1</sup>, D. Gandolfi<sup>13</sup>, M. Gillon<sup>25</sup>, M. Güdel<sup>28</sup>, P. Gutermann<sup>5,29</sup>, J. Hasiba<sup>15</sup>, K. G. Isaak<sup>23</sup>, L. Kiss<sup>30</sup>, J. Laskar<sup>31</sup>, A. Lecavelier des Etangs<sup>32</sup>, C. Lovis<sup>1</sup>, D. Magrin<sup>14</sup>, P. F. L. Maxted<sup>33</sup>, M. Munari<sup>34</sup>, V. Nascimbeni<sup>14</sup>, R. Ottensamer<sup>28</sup>, I. Pagano<sup>34</sup>, E. Pallé<sup>11</sup>, G. Peter<sup>35</sup>, G. Piotto<sup>14,36</sup>, D. Pollacco<sup>9</sup>, D. Queloz<sup>37,38</sup>, R. Ragazzoni<sup>14,36</sup>, N. Rando<sup>23</sup>, H. Rauer<sup>21,39,40</sup>, I. Ribas<sup>17,41</sup>, N. C. Santos<sup>7,8</sup>, G. Scandariato<sup>34</sup>, D. Ségransan<sup>1</sup>, A. E. Simon<sup>2</sup>, A. M. S. Smith<sup>21</sup>, M. Steller<sup>15</sup>, Gy. M. Szabó<sup>42,43</sup>, N. Thomas<sup>2</sup>, S. Udry<sup>1</sup>, I. Walter<sup>35</sup>, and N. Walton<sup>44</sup>

(Affiliations can be found after the references)

Received January 1, 2021; accepted January 1, 2021

### ABSTRACT

**Context.** Gas giants orbiting close to hot and massive early-type stars can reach dayside temperatures that are comparable to those of the coldest stars. These “ultra-hot Jupiters” have atmospheres made of ions and atomic species from molecular dissociation and feature strong day-to-night temperature gradients. Photometric observations at different orbital phases provide insights on the planet atmospheric properties.

**Aims.** We analyse the photometric observations of WASP-189 acquired with the instrument CHEOPS to derive constraints on the system architecture and the planetary atmosphere.

**Methods.** We implement a light curve model suited for asymmetric transit shape caused by the gravity-darkened photosphere of the fast-rotating host star. We also model the reflective and thermal components of the planetary flux, the effect of stellar oblateness and light-travel time on transit-eclipse timings, the stellar activity and CHEOPS systematics.

**Results.** From the asymmetric transit, we measure the size of the ultra-hot Jupiter WASP-189 b,  $R_p = 1.600^{+0.017}_{-0.016} R_J$ , with a precision of 1%, and the true orbital obliquity of the planetary system  $\Psi_p = 89.6 \pm 1.2$  deg (polar orbit). We detect no significant hotspot offset from the phase curve and obtain an eclipse depth  $\delta_{\text{ecl}} = 96.5^{+4.5}_{-5.0}$  ppm, from which we derive an upper limit on the geometric albedo:  $A_g < 0.48$ . We also find that the eclipse depth can only be explained by thermal emission alone in the case of extremely inefficient energy redistribution. Finally, we attribute the photometric variability to the stellar rotation, either through superficial inhomogeneities or resonance couplings between the convective core and the radiative envelope.

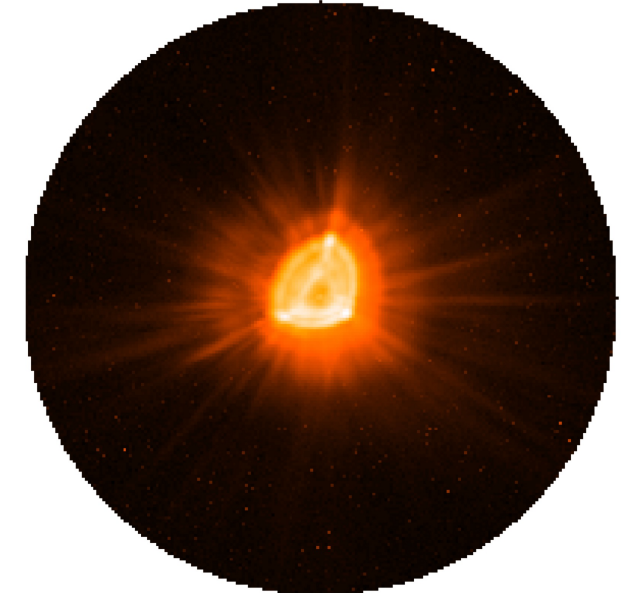
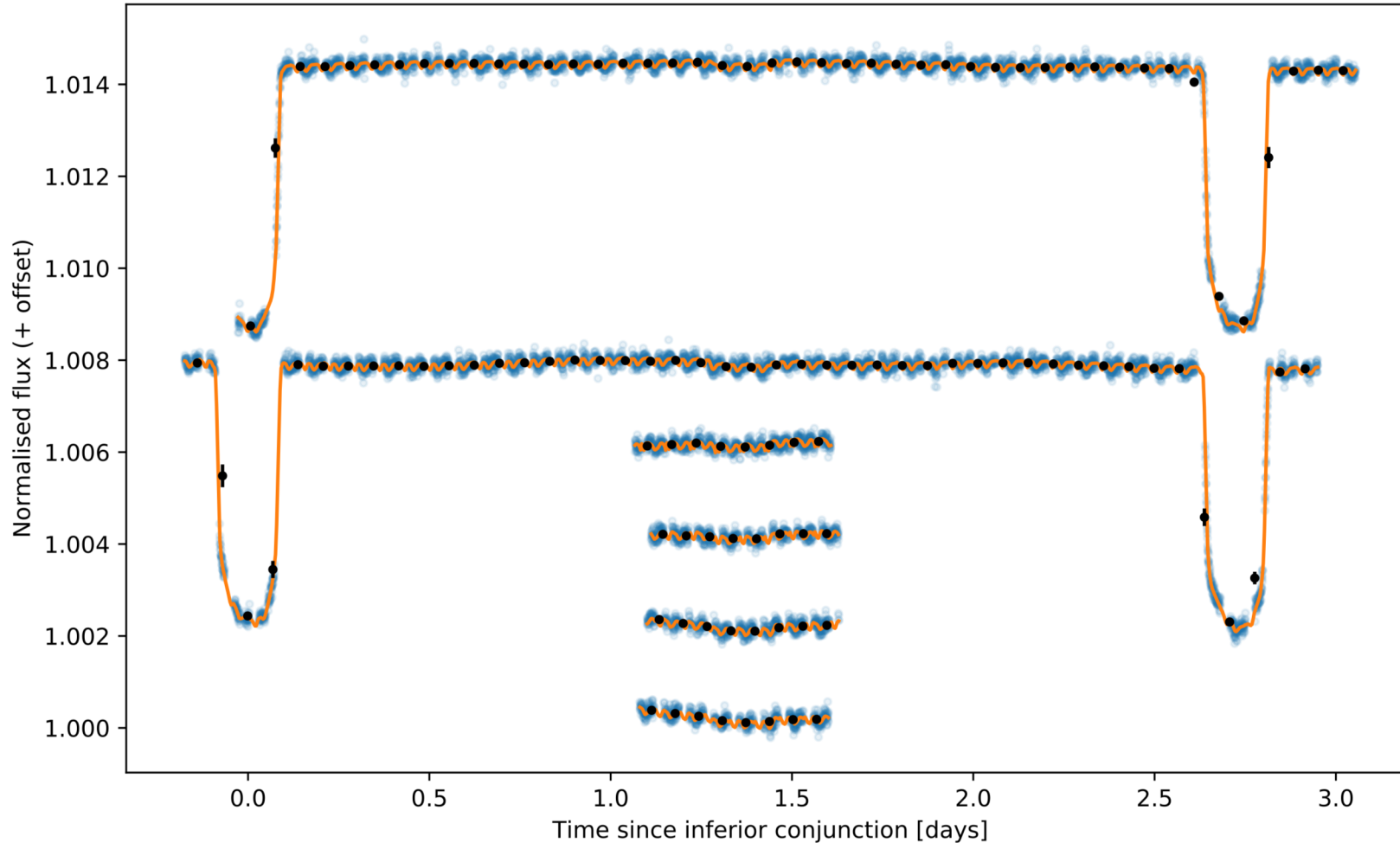
**Conclusions.** Based on the derived system architecture, we predict the eclipse depth in the upcoming TESS observations to be up to  $\sim 165$  ppm. High-precision detection of the eclipse in both CHEOPS and TESS passbands might help disentangle between reflective and thermal contributions. We also expect the right ascension of the ascending node of the orbit to precess due to the perturbations induced by the stellar quadrupole moment  $J_2$  (oblateness).

**Key words.** techniques: photometric – planets and satellites: atmospheres – planets and satellites: individual: WASP-189 b

Accepted for publication in A&A

Available on arXiv: [arXiv:2201.04518](https://arxiv.org/abs/2201.04518)

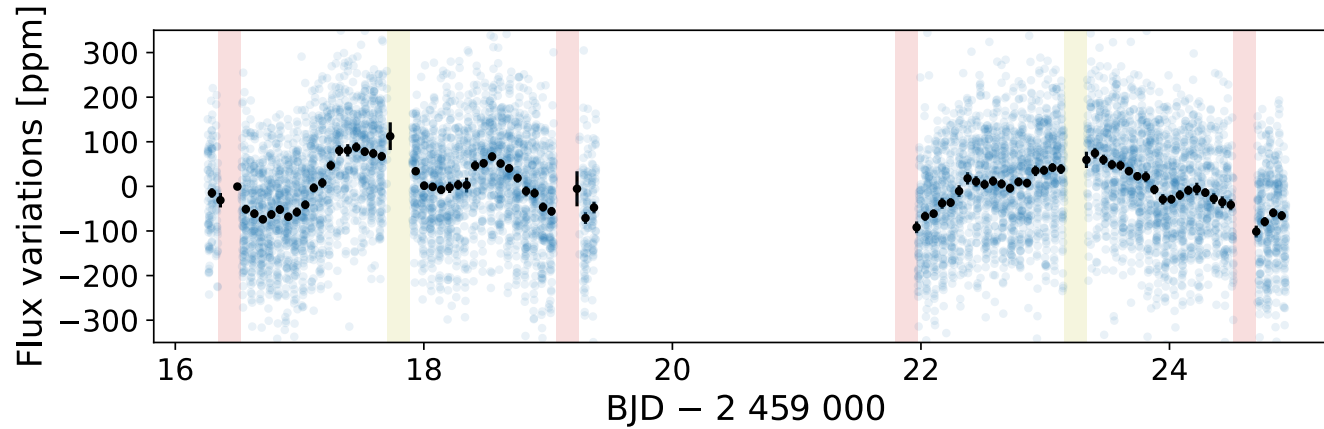
# CHEOPS observations



4 occultations  
(reported in Lendl et al. 2020)

2 full planetary orbits  
(incl. 2 transits reported in Lendl et al. 2020)

# Stellar activity

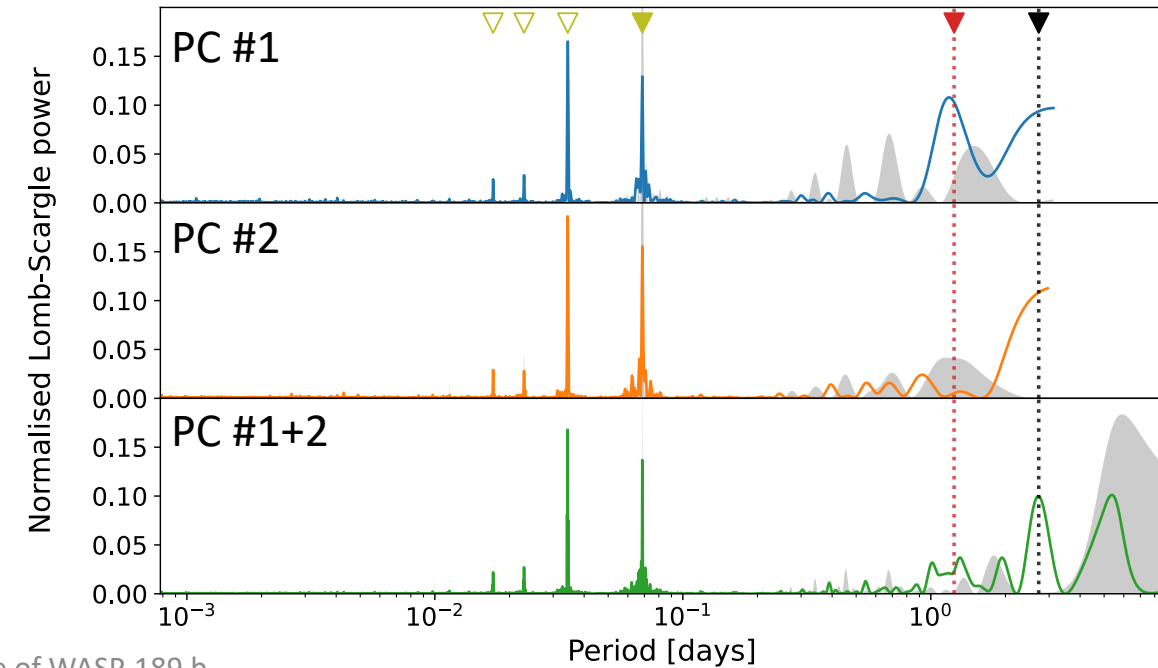


Phase curve #1: **strong** photometric variability

Phase curve #2: *weak* photometric variability

➔ **PC#1 periodicity matches stellar rotation**

- ▶ CHEOPS orbital period
  - ▶ Stellar rotation period (*Lendl et al. 2020*)
  - ▶ WASP-189b orbital period
- Spectral window function*

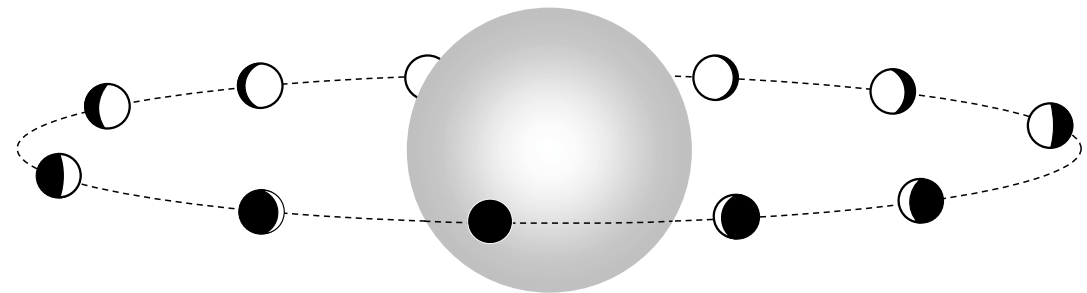


# Global model

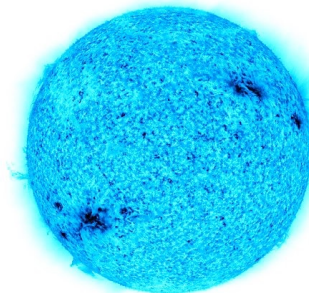
- Systematic noise
  - field of view rotation
  - thermo-mechanical "ramp" effect
  - linear and quadratic long-term trend
- Planetary model
  - Transit model with a gravity-darkened star
  - Eclipse model with an oblate star
  - Phase curve signal
- Stellar variability in the phase curves
  - Gaussian process with quasi-periodic kernel



© ESA/ATG



Winn (2011)



# Planetary model: transit model

- Gravity-darkened oblate star modelled with **pytransit\*** (Parviainen 2015)

- Stellar local flux:

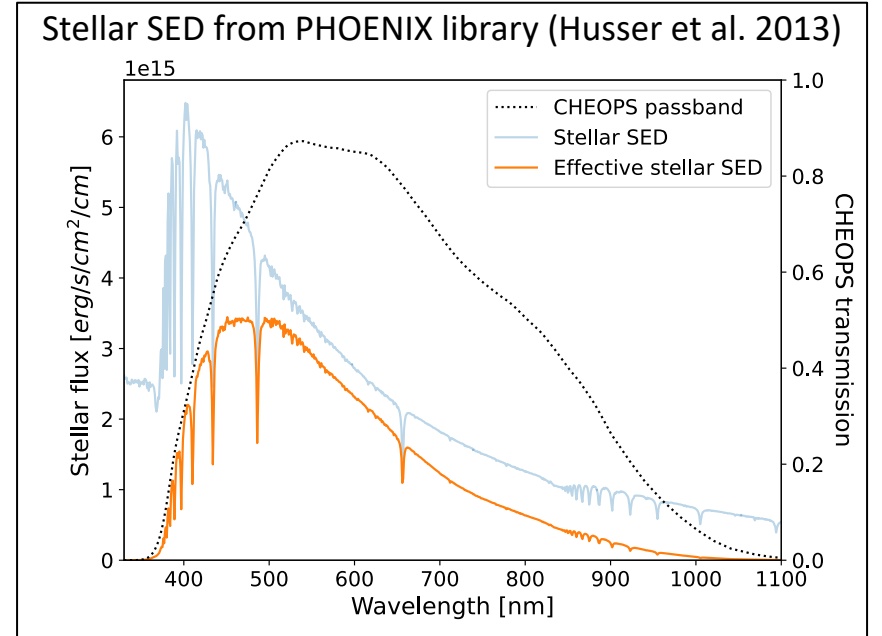
$$T(\vartheta) = T_{\text{pole}} \left( \frac{g_{\text{eff}}(\vartheta)}{g_{\text{eff, pole}}} \right)^\beta \quad \vec{g}_{\text{eff}}(\vartheta) = -\frac{G M_\star}{r_\vartheta^2} \vec{u}_r + \left( \frac{2\pi}{P_\star} \right)^2 R_\star \sin(\vartheta) \vec{u}_x$$

$$\mathcal{F}(\vartheta, \mu) = \int_{\lambda=0}^{+\infty} S(\lambda, T(\vartheta)) \mathcal{T}_{\text{inst}}(\lambda) d\lambda \times \mathcal{I}(\mu)$$

*Stellar SED*  
*CHEOPS passband*  
*Limb-darkening law*

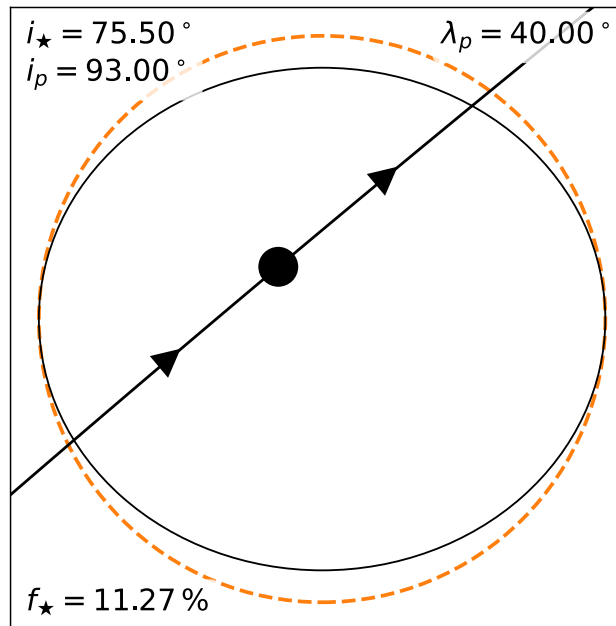
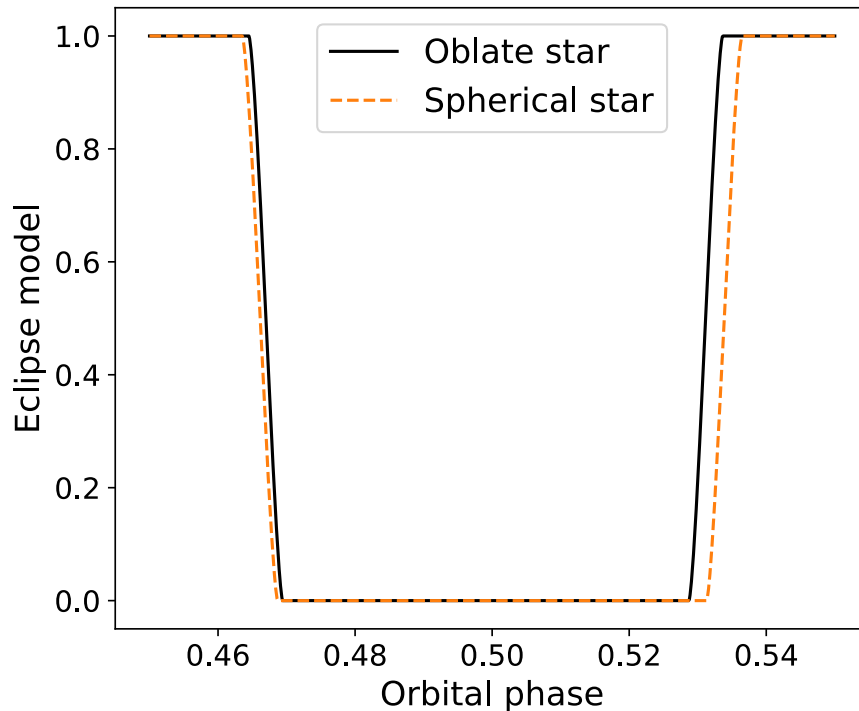
- Stellar oblateness:

$$f_\star = 1 - \frac{R_{\text{pole}}}{R_\star} = \frac{2\pi^2 R_\star^3}{2\pi^2 R_\star^3 + G M_\star P_\star^2} = \frac{3\pi}{2 G \rho_\star P_\star^2}$$



\* <https://github.com/hpparvi/PyTransit>

# Planetary model: eclipse model



Accounting for stellar oblateness:  
model computed  
using a **pytransit** transit model  
in front of a uniform stellar disc

Same parameters as for the transit  
except the following transformation:

$$\begin{aligned}\omega_{\text{ecl}} &= \omega + 180^{\circ} \\ i_{p,\text{ecl}} &= 180^{\circ} - i_p \\ \lambda_{p,\text{ecl}} &= -\lambda_p\end{aligned}$$

# Planetary model: phase curve signal

- Reflected light from a Lambertian sphere (Sobolev 1975; Charbonneau et al. 1999)

$$\frac{F_{\text{refl}}}{F_{\star}} = A_g \left( \frac{R_p}{a} \frac{1 + e \cos(\nu)}{1 - e^2} \right)^2 \frac{\sin(\alpha) + (\pi - \alpha) \cos(\alpha)}{\pi}$$

$\alpha$ : phase angle of the planet

- Thermal emission:

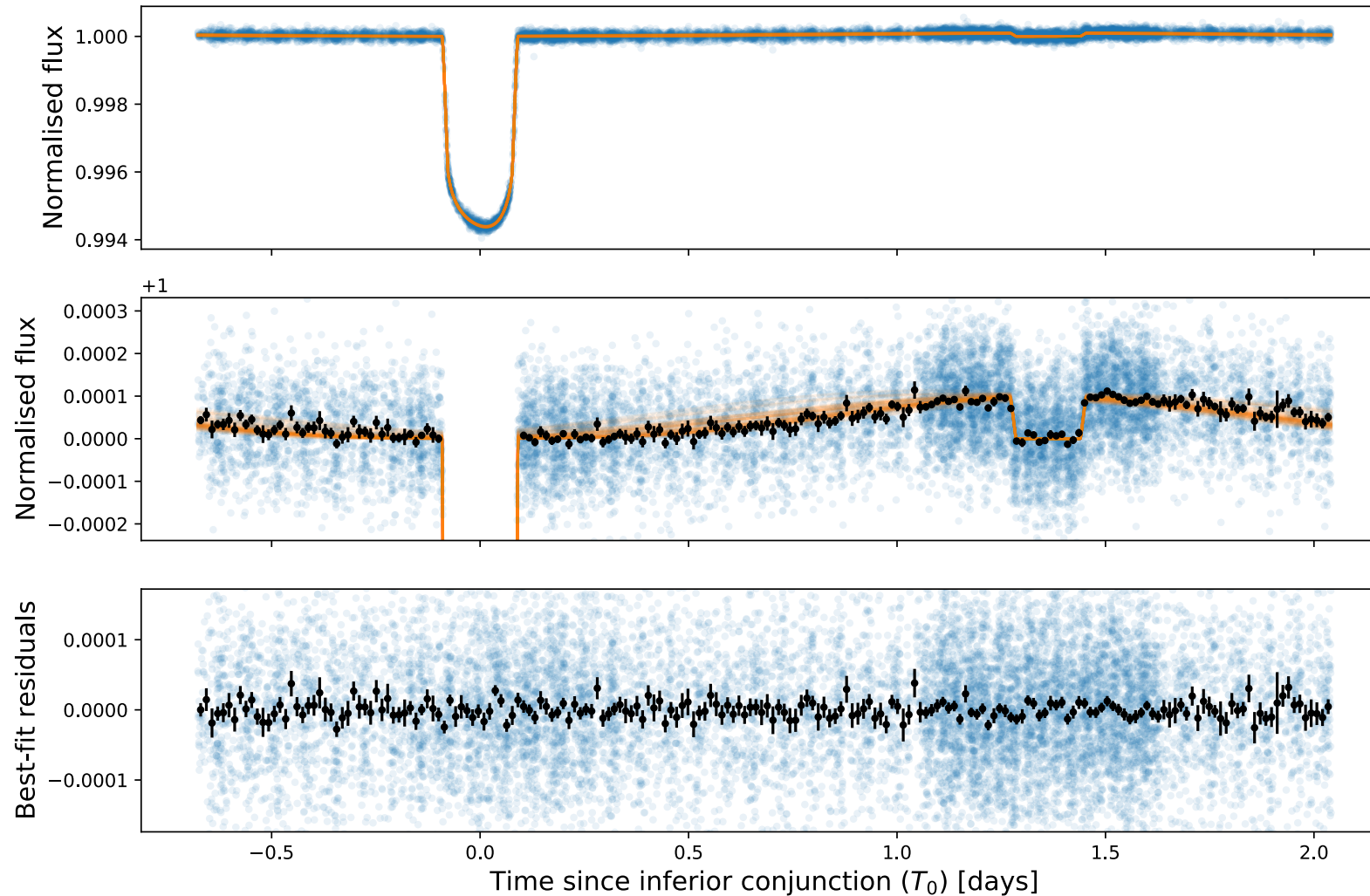
$$F_{\text{therm}} = (F_{\text{day}} - F_{\text{night}}) \frac{1 + \cos(\alpha_{\text{therm}})}{2} + F_{\text{night}}$$

$$\alpha_{\text{therm}} = \arccos\left[-\sin(\omega + \nu - \phi_{\text{therm}}) \sin(i_p)\right]$$

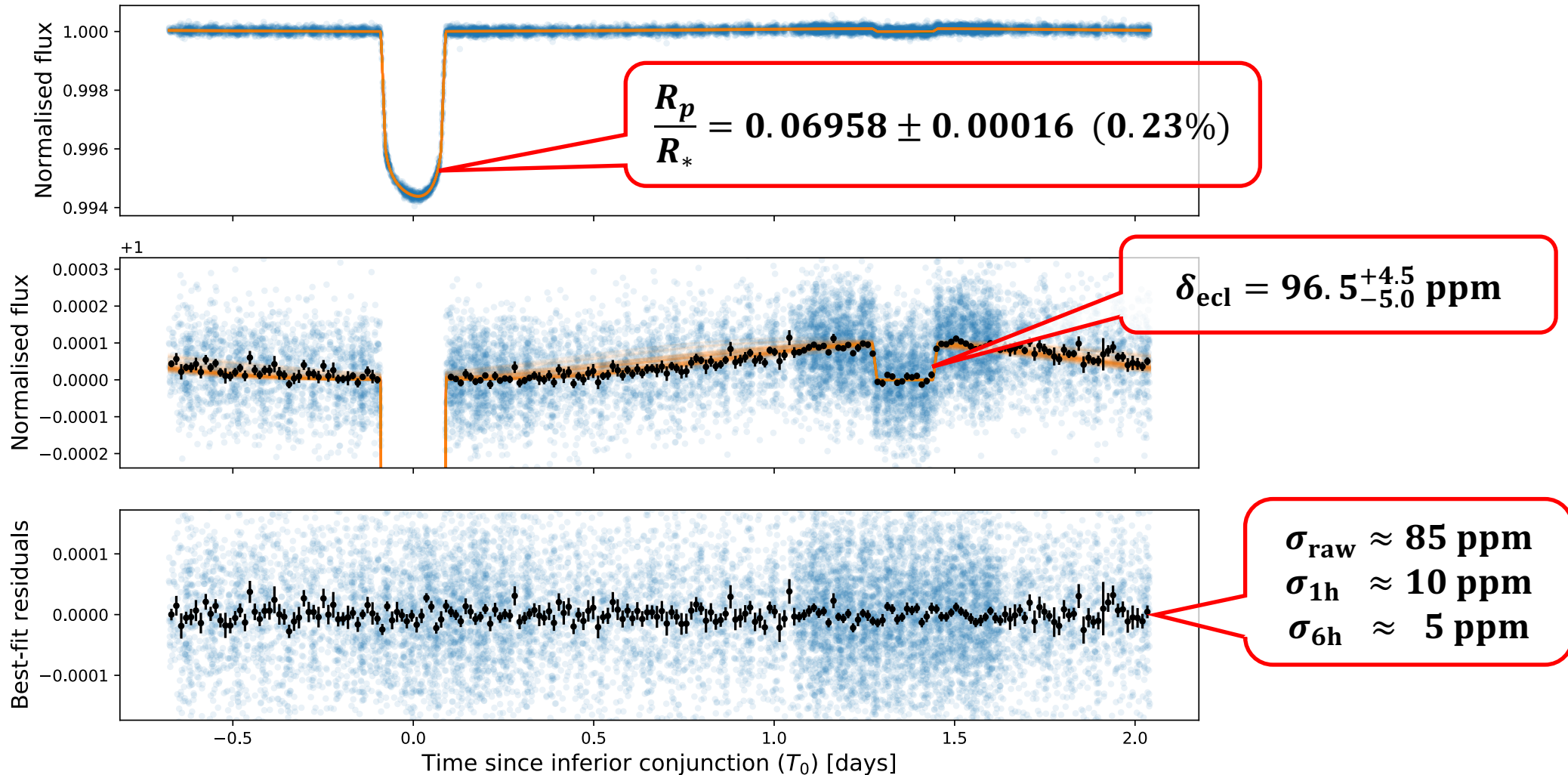
- Ellipsoidal variations and Doppler beaming:
  - options not included after BIC- and AIC-based model comparison

*Light-travel time (up to 50 sec) accounted for in both eclipse and phase curve models*

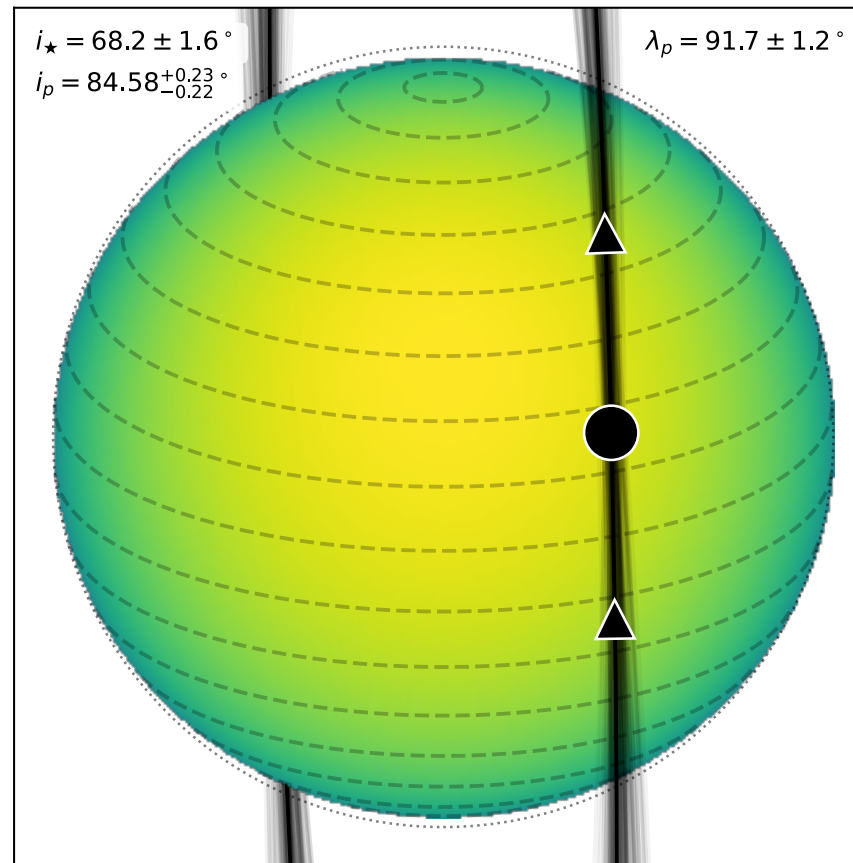
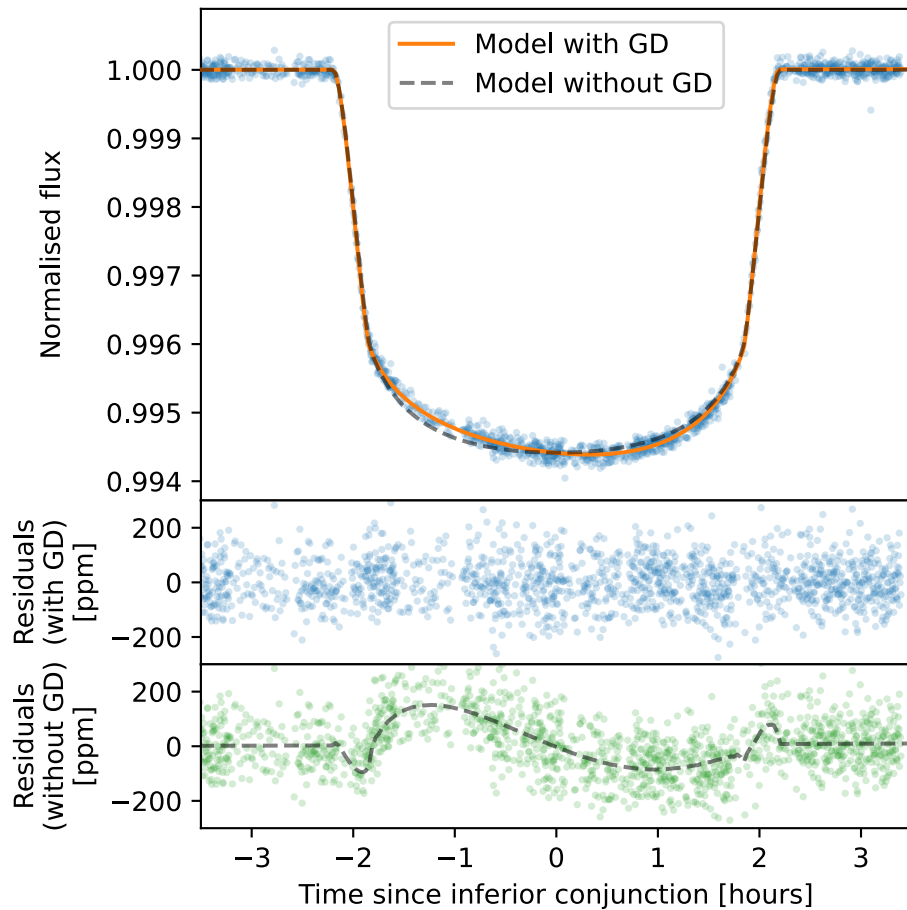
# Detrended phase curve



# Photometric precision

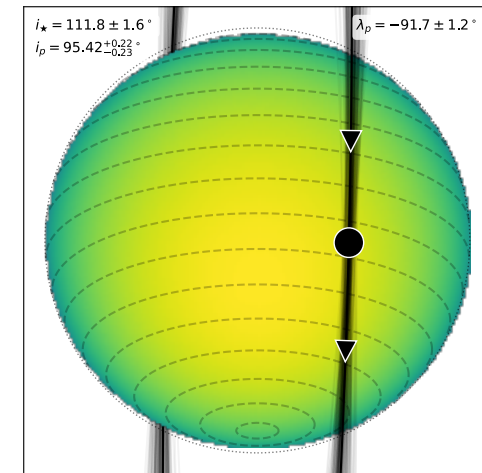


# Transit asymmetry and system architecture



$$f_* = 2.88^{+0.15}_{-0.12} \%$$

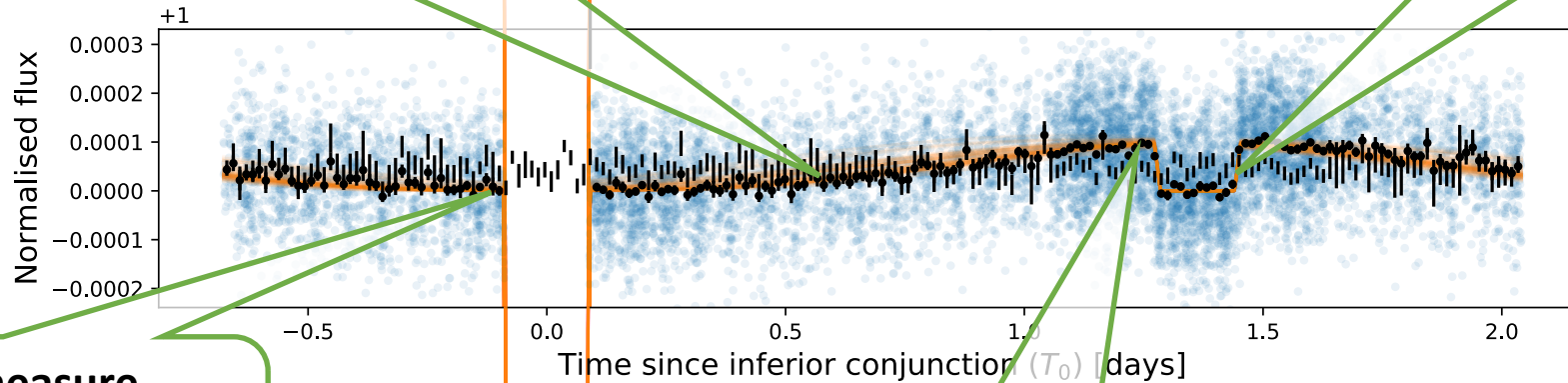
$$\Psi_p = 89.6 \pm 1.2^\circ$$



# Phase curve and atmospheric properties

Large uncertainty on the phase curve compared to the transit/eclipse events

$$\delta_{\text{ecl}} = 96.5^{+4.5}_{-5.0} \text{ ppm}$$



Unable to measure the nightside flux due to stellar variability



No constraint on heat redistribution efficiency

No significant hotspot offset  
 $\phi_{\text{therm}} = -7 \pm 17^\circ$



Strong degeneracy between reflected light and thermal emission components

# Phase curve and atmospheric properties

**Unable to disentangle the contributions  
of reflected light and thermal emission**

Search for upper/lower limits in two extreme scenarios:

- 1) phase curve amplitude due to reflected light only
- 2) phase curve amplitude due to thermal emission only

# Atmospheric properties – reflected light

$$\delta_{\text{ecl}} = \frac{F_p}{F_*} = A_g \left( \frac{R_p}{a} \right)^2 \Rightarrow A_{g,\text{max}} = 0.42 \pm 0.02$$

$$\boxed{A_g < \mathbf{0.48}} \text{ (99.93\% confidence)}$$

*No constraint on any deviation from a Lambertian reflector*

# Atmospheric properties – thermal emission

- Effective average temperature of the planet:

$$\tilde{T}_p^4 = \frac{1 - A_B}{4 \sigma_{\text{SB}}} \left( \frac{R_\star}{a} \right)^2 \int_{\lambda=0}^{+\infty} \mathcal{S}(\lambda, T_\star) d\lambda$$

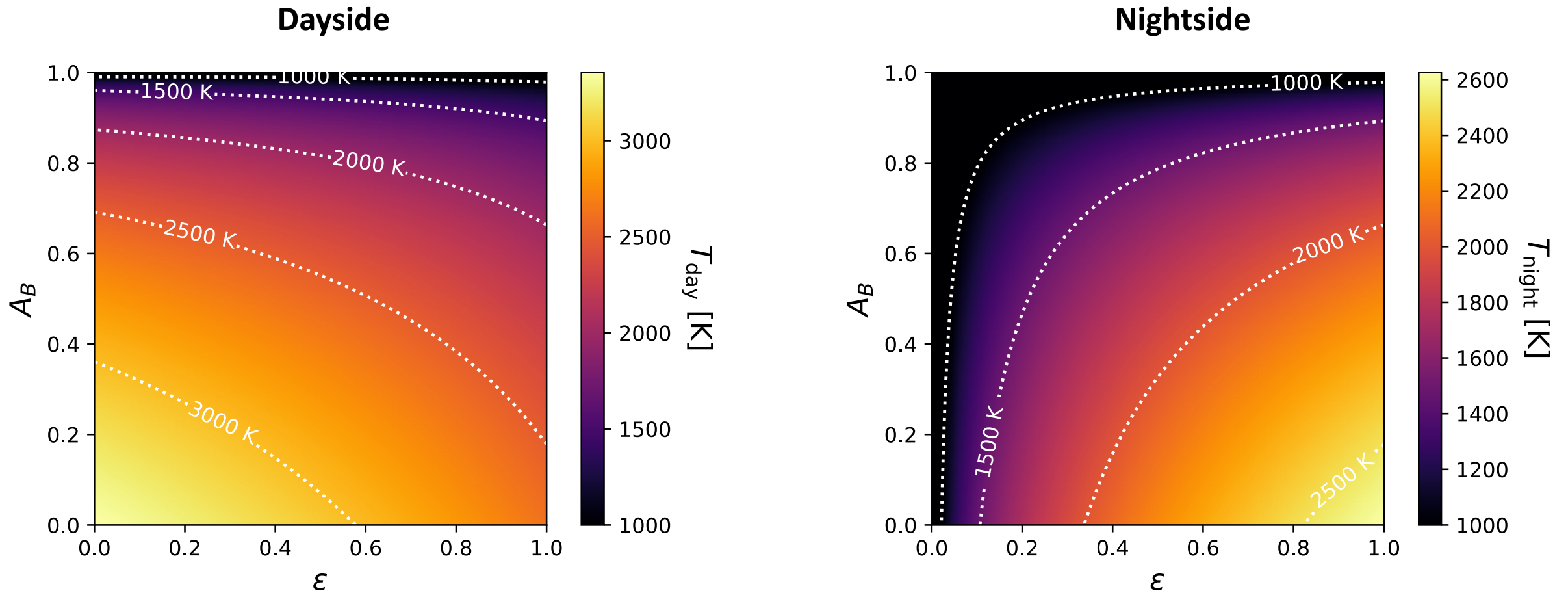
- Following Cowan & Agol (2011):

$$T_{\text{day}} = \left( \frac{8 - 5\varepsilon}{3} \right)^{\frac{1}{4}} \tilde{T}_p \quad T_{\text{night}} = \varepsilon^{\frac{1}{4}} \tilde{T}_p$$

- Eclipse depth from the  $T_{\text{day}}$ :

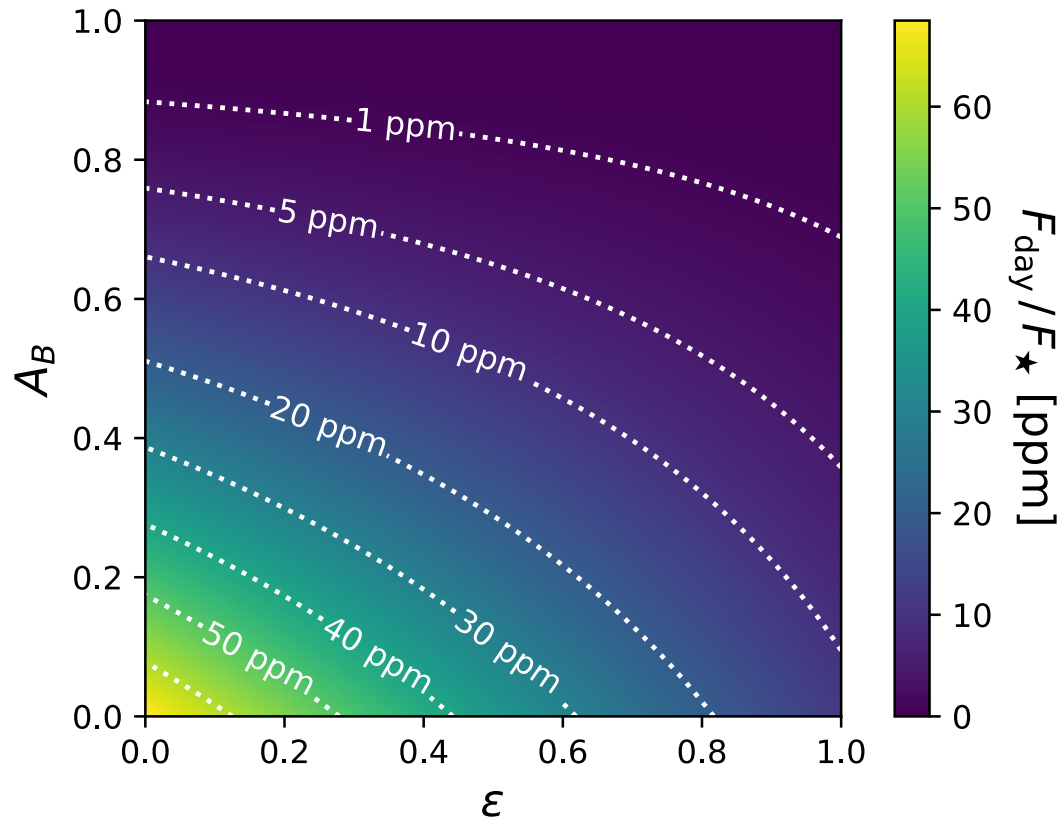
$$\frac{F_{\text{day}}}{F_\star} = \left( \frac{R_p}{R_\star} \right)^2 \frac{\int_{\lambda=0}^{+\infty} \mathcal{S}(\lambda, T_{\text{day}}) \mathcal{T}_{\text{inst}}(\lambda) d\lambda}{\int_{\lambda=0}^{+\infty} \mathcal{S}(\lambda, T_\star) \mathcal{T}_{\text{inst}}(\lambda) d\lambda}$$

# Atmospheric properties – thermal emission



# Atmospheric properties – thermal emission

Flux in CHEOPS passband



Max. eclipse depth =  $68.5 \pm 1.8$  ppm

Not enough to explain measured eclipse depth

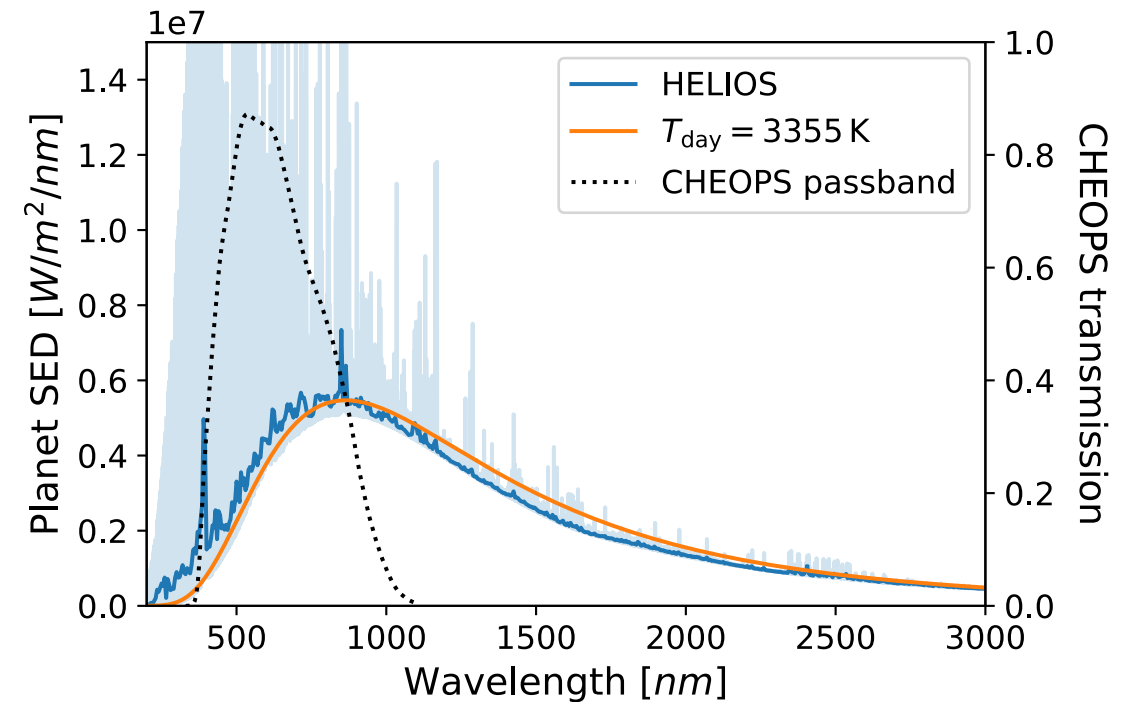
Assuming a black body,  $T_{\text{day}}$  must be  $3542 \pm 14$  K  
but this means  $A_B \approx -0.24$  for  $\epsilon = 0$

See Sect. 3.3 of **Morris et al. (2021)**  
for a discussion about negative Bond albedo values  
([arXiv:2110.11837](https://arxiv.org/abs/2110.11837))

# Atmospheric properties – thermal emission

- Computing a synthetic emission spectrum for the planet using **HELIOS** (Malik et al. 2017, 2019)
- Pushing other parameters to the limits (*smallest and coolest star*)
- Max thermal flux with  $A_B = 0$ :  
 $87.1 \pm 3.1$  ppm (1.6 $\sigma$  consistency)

$$\rightarrow A_g > 0.041 \pm 0.026$$

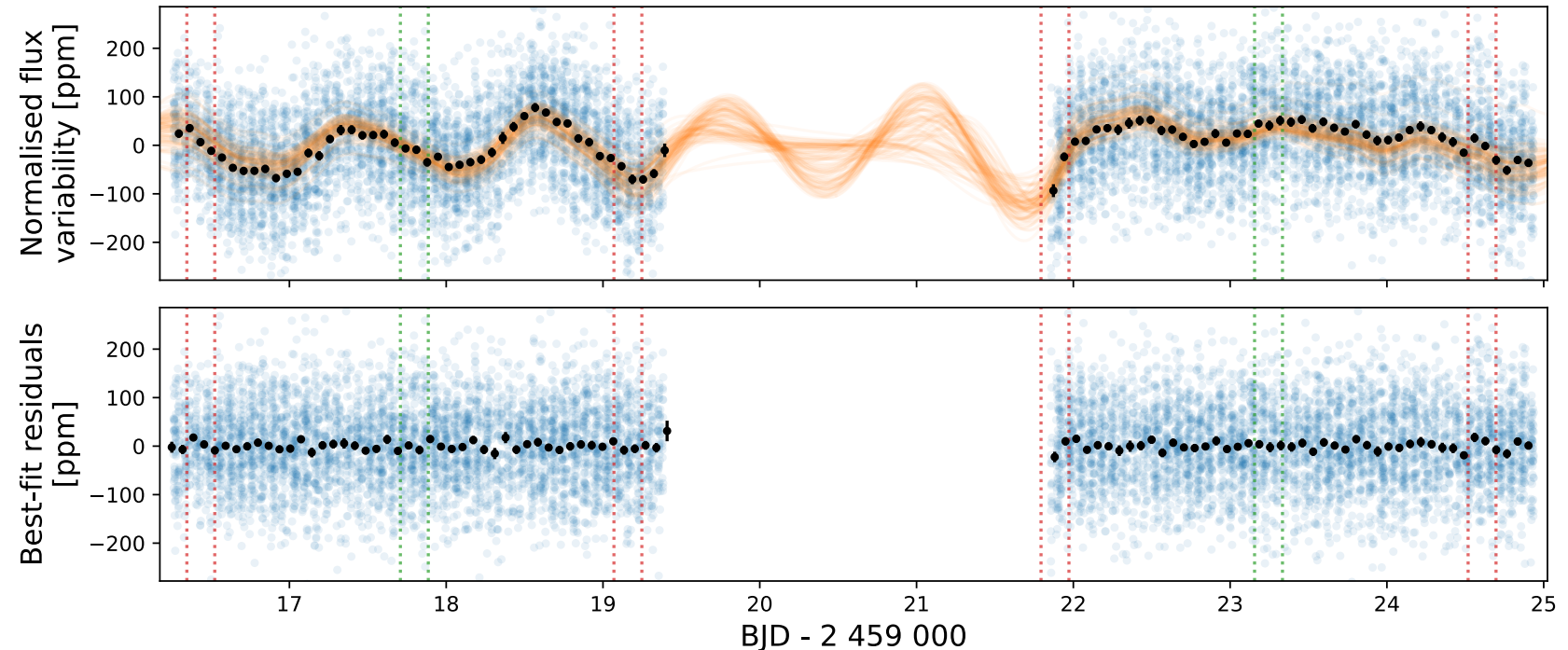


# Stellar activity

Photometric variability matching stellar rotation

$$P_{\star} = 1.198^{+0.026}_{-0.025} \text{ days}$$

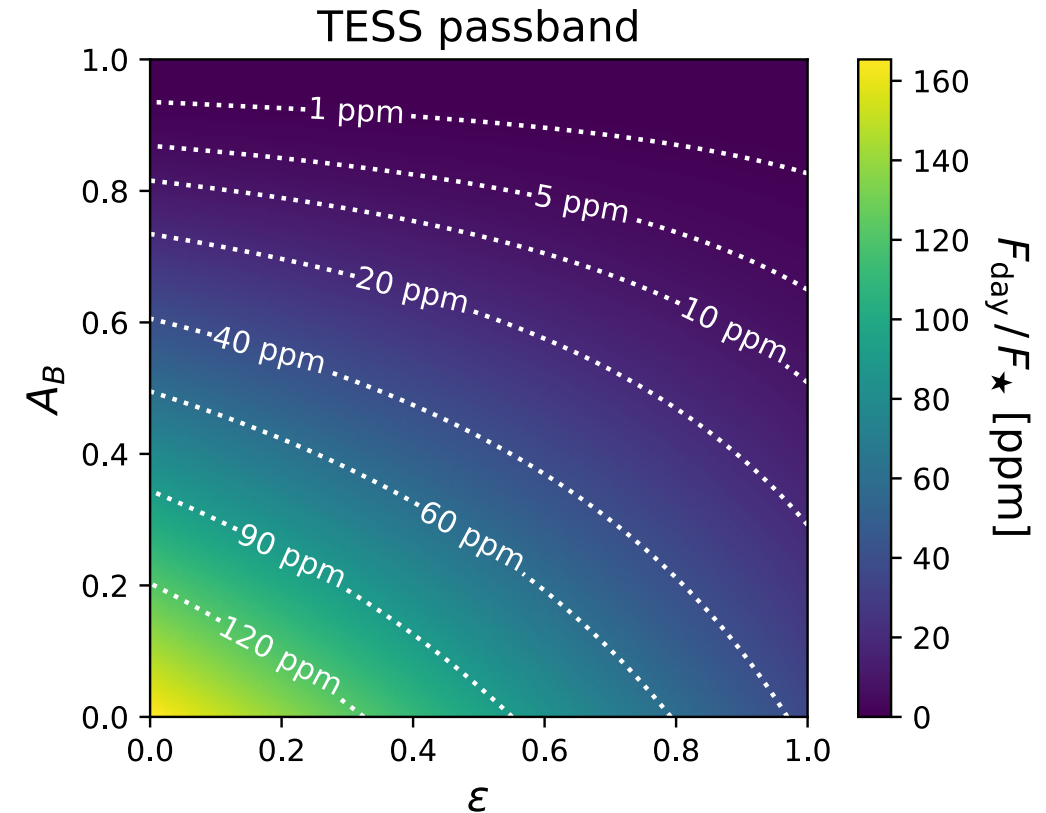
WASP-189 at the limit of convective/radiative outer envelope  
(*Fossati et al. 2018*)



- Convective scenario:
  - stellar spots
- Radiative scenario
  - inhomogeneities of unknown origin at the surface of hot stars (*Trust et al. 2020*)
  - non-radial pulsations excited through resonance couplings between convective core and radiative envelope (*Lee & Saio 2020*)

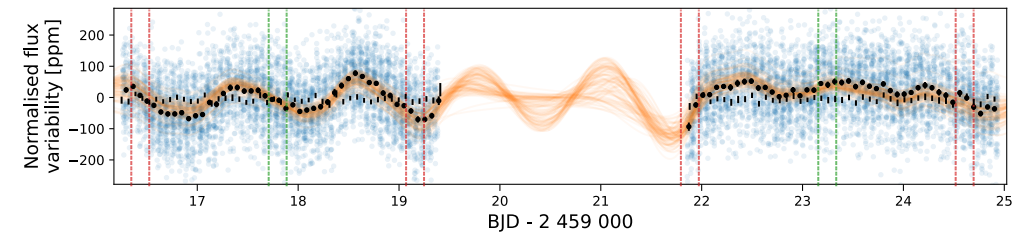
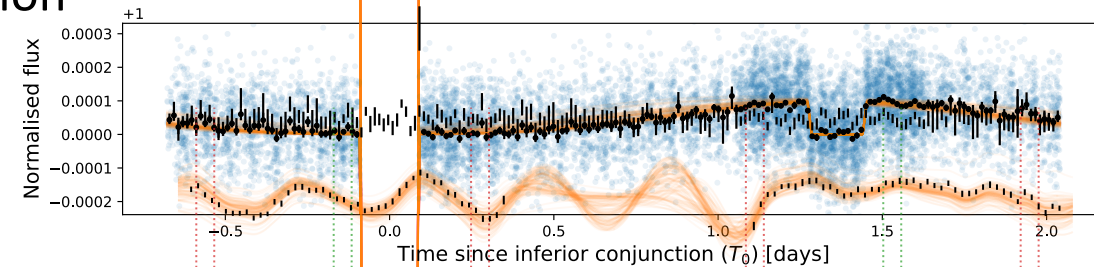
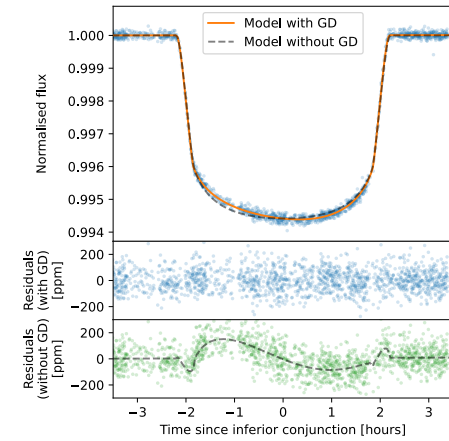
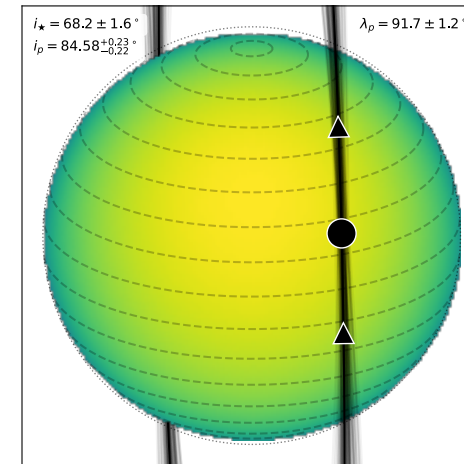
# TESS observation is coming

- Sector 51 (April/May 2022)
- Eclipse depth up to 165 ppm
- Stellar variability better characterised
- Joint analysis with CHEOPS data to help disentangling thermal and reflective components  
*(assuming both instruments probe the same atmospheric layer)*



# Summary

- Refined planetary parameters
- System architecture constrained (polar orbit)
- No hotspot offset detected
- Degeneracy between reflected light and thermal emission
  - $A_g < 0.48$
  - $A_g > 0.041 \pm 0.026$  ( $A_B = 0$ )
- Stellar activity detected
  - Stellar spots
  - Core-envelope resonance couplings
- TESS-CHEOPS light curves to constrain thermal emission





UNIVERSITÉ  
DE GENÈVE

FACULTÉ DES SCIENCES  
Département d'astronomie



The atmosphere and architecture  
of WASP-189 b  
probed by its **CHEOPS** phase curve

*Thank you for your attention !  
Questions?*